Charge transfer in collisions of O^+ with H and H^+ with O

P.C. Stancil[1,2], **D.R. Schultz**[1], **M. Kimura**[3], **J.-P. Gu**[4], **G. Hirsch**[4,†] **and R.J. Buenker**[4]

[1] Physics Division, Oak Ridge National Laboratory, P.O. Box 2008, Oak Ridge, TN 37831-6372, U.S.A.
   e-mail: stancil@mail.phy.ornl.gov, schultz@mail.phy.ornl.gov

[2] Department of Physics and Astronomy, University of Tennessee, Knoxville, TN 37996-1200, U.S.A.

[3] Graduate School of Science and Engineering, Yamaguchi University, Ube, Yamaguchi 755, Japan
   e-mail: mineo@rikaxp.riken.go.jp

[4] Theoretische Chemie, Bergische Universität-Gesamthochschule Wuppertal, Gaußstr. 20, D-42097 Wuppertal, Germany
   e-mail: jgu@ist.ucf.edu, buenker@wrcs1.urz.uni-wuppertal.de

Received June 29; accepted September 20, 1999

Abstract. Cross sections and rate coefficients for total and fine-structure resolved charge transfer in collisions of O^+ with H and H^+ with O are presented for collision energies between 0.1 meV/u and 10 MeV/u and temperatures between 10 and 10^7 K. The results are obtained utilizing new quantal and semiclassical molecular-orbital close-coupling, classical trajectory Monte Carlo, and continuum distorted wave calculations in conjunction with previous experimental and theoretical data. Applications to various astrophysical and atmospheric environments are discussed.
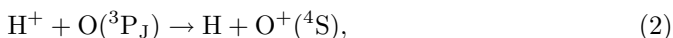
Key words: atomic processes — ISM: atoms — interplanetary medium — comets: general — planets and satellites: individual: Jupiter

1. Introduction

Electron capture by oxygen ions due to collisions with neutral hydrogen,

$$O^+(^4S) + H \rightarrow O(^3P_J) + H^+, \qquad (1)$$
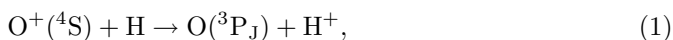
and the reverse process,

$$H^+ + O(^3P_J) \rightarrow H + O^+(^4S), \qquad (2)$$

are known to play important roles in a variety of astrophysical, atmospheric, and laboratory plasmas because of the relatively large abundances of the collision partners and the accidental near degeneracy of the hydrogen and oxygen ionization potentials. As processes (1) and (2) are quasi-resonant, their cross sections are large, from the thermal to intermediate energy regimes. Both

reactions have received considerable experimental and theoretical attention, but all the previous studies have determined the cross sections for collision energies greater than ~ 1 eV/u except for the quantal molecular-orbital close-coupling (MOCC) calculation of Chambaud et al. (1980), which covered the energy range ~ 0.02 to 0.45 eV/u and the semiclassical calculations of Rapp & Ortenburger (1960). For process (1), the lowest experimental point is at 1.6 eV/u (Fite et al. 1962). Rutherford & Vroom (1974) obtained the lowest experimental energy of 2 eV/u for reaction (2).

For most astrophysical applications, the important quantity is the rate coefficient. Rate coefficients for reactions (1) and (2) have been calculated by Field & Steigman (1971) for $T = 10 - 10000$ K and by Chambaud et al. (1980) for $T = 10 - 1000$ K. Kimura et al. (1997) computed rate coefficients for reaction (2) for $T = 10000 - 200000$ K. The results of Chambaud et al. (1980), which are confirmed by the drift-tube measurements of reaction (2) by Federer et al. (1984) for $T \sim 1000$ K, are in significant disagreement with Field & Steigman (1971).

In an attempt to resolve these discrepancies, we have combined new theoretical calculations, using four different approaches applicable in different energy regimes, with previous experimental and theoretical results, to deduce accurate charge transfer cross sections and rate coefficients for processes (1) and (2). Brief descriptions of the scattering theories are given in Sect. 2. New results and comparison with previous data are presented in Sect. 3 with the cross sections given over the very large energy range, 0.1 meV/u − 10 MeV/u, the higher energies being of relevance to ion precipitation into the Jovian atmosphere. This and other applications of the results to astrophysical and atmospheric environments are discussed in Sect. 4.

Send offprint requests to: P.C. Stancil
   † Deceased.

2. Scattering theory

As there is currently no theoretical approach which is applicable over the full energy range considered, processes (1) and (2) are investigated with four different methods each applicable in different, but generally overlapping, energy regimes. The intercomparison of the various theoretical approaches gives a measure of their accuracy and reliability as do comparisons with other theoretical and experimental data. A similar approach was successfully applied to the $C^+ + H$ and $H^+ + C$ collision systems (Stancil et al. 1998a, 1998b).

For collision energies less than ~10 keV/u, one of the most robust approaches, the molecular-orbital close-coupling (MOCC) method (e.g., Kimura & Lane 1990; Zygelman et al. 1992) was utilized incorporating the potential energy curves and nonadiabatic coupling matrix elements of Kimura et al. (1997). Table 1 lists the three molecular states included in the calculations and their experimental separated-atom energies. The collisional dynamics are solved in a semiclassical formalism including electron translation factors (ETFs) for energies between 1 eV/u and 10 keV/u and quantum-mechanically between 0.1 and 500 eV/u.

For collision energies less than ~ 0.5 eV/u, the fine-structure of the oxygen atom must be considered. The quantal MOCC method is extended to include the fine-structure levels following the approach of Chambaud et al. (1980) (see also Roueff & Dalgarno 1988). As in Chambaud et al. we included the $1\ ^3\Sigma^- - 2\ ^3\Sigma^-$ radial coupling, but neglected rotational coupling which was found to have a negligible effect in the three channel, fine-structure unresolved MOCC calculations. Spin-orbit coupling was included, but assumed to be independent of internuclear distance and equal to the experimental separated-atom energies given in Table 1. The fine-structure quantum MOCC (QMOCC-FS) calculation involved 12 scattering channels divided into two uncoupled blocks of five and seven channels of opposite total parity.

For collision energies greater than 5 keV/u, the cross sections were computed with the classical trajectory Monte Carlo (CTMC) method (e.g., Olson & Salop 1977). CTMC has been shown to be reliable for a wide range of intermediate energies, but may not be accurate at low energies as it yields essentially a classical over-the-barrier result and neglects charge transfer by tunneling of the electron through the barrier. Further, to apply CTMC to multielectron projectiles, such as O^+, traditional effective nuclear charge techniques used for single- and few-electron systems were found to be unsuitable. To address this problem we have developed an approach which utilizes a binding-energy-dependent effective charge deduced from standard atomic spectroscopic data to model the electronic structure of the projectile following capture. This approach is described in Schultz & Stancil (1999) along

Table 1. Asymptotic separated-atom energies of OH^+

Molecular States	Asymptotic Atomic States	Energy[a] (K)	(meV)
$1\ ^3\Sigma^-, 1\ ^3\Pi$	$O(^3P_2) + H^+$	0	0
	$O(^3P_1) + H^+$	228	19.7
	$O(^3P_0) + H^+$	326	28.1
$2\ ^3\Sigma^-$	$O^+(^4S) + H$	227	19.6

[a] Bashkin & Stoner (1975).

with state-dependent n, l charge transfer cross sections needed for studies of radiative emission following charge transfer of precipitating ions in the Jovian atmosphere.

To treat electron capture from the inner orbitals of O by proton impact, the CTMC model was extended (Schultz & Stancil 1999) to include a constraining potential, enforcing a quantal representation of the ground state. At higher impact energies, capture from the O K-shell dominates and is otherwise significantly overestimated by the standard CTMC approach. This improved approximation is needed to benchmark state-selective charge transfer cross sections, not readily obtainable with other intermediate-energy methods.

The continuum distorted wave (CDW) method is used for high energies utilizing the methods of Belkić et al. (1984). The target and projectile atomic wave functions are described by linear combinations of Slater type orbitals taken from Clementi & Roetti (1974). The method should be reliable for collision energies greater than ~500 keV/u.

3. Results and discussion

The total cross sections for reaction (1) computed in this work are presented in Fig. 1 along with all the available experimental data, previous calculations, and the recommended cross section of Janev et al. (1995). The quantal MOCC (QMOCC) calculations are in good agreement with the measurements of Stebbings et al. (1960) and Fite et al. (1962). Between ~ 0.2 and ~ 1 eV/u a rapid oscillation is apparent in the QMOCC cross section (see also Fig. 2). This may be due to orbiting effects in the very shallow bound potential of the OH^+ $2\ ^3\Sigma^-$ state which is further discussed in Krajcar-Bronic et al. (1999). The current QMOCC calculation included three electronic channels with the energy difference of 115 K (9.91 meV), obtained from the centroid of the O fine-structure levels (see Table 1). It was found that radial coupling was the dominant charge transfer mechanism with rotational coupling giving a negligible contribution.

Figure 1 also shows our semiclassical MOCC (SCMOCC) which is in excellent agreement with the measurements of Stebbings et al. (1960), Fite et al. (1962), and Phaneuf et al. (1978), while the semiclassical
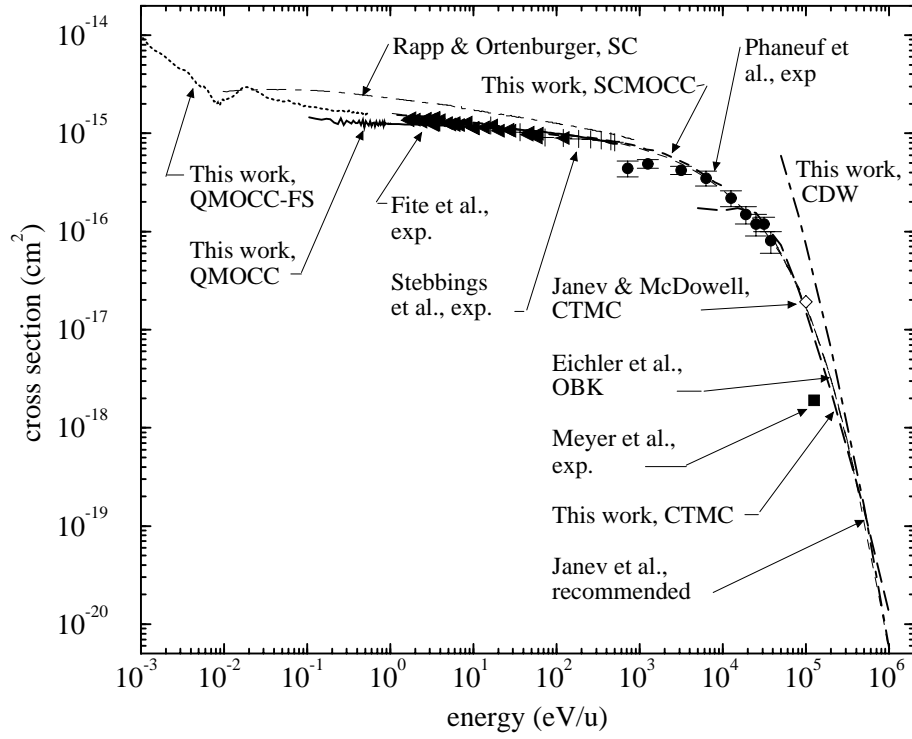
Fig. 1. Total charge transfer cross sections for reaction (1), O$^+$ + H → O + H$^+$. This work: QMOCC [thick solid line], QMOCC-FS [thick dotted line], SCMOCC [thick dashed line], CTMC [thick long dashed line], CDW [thick dot-dashed line]. Previous experiment: Stebbings et al. (1960) [pluses], Fite et al. (1962) [filled left triangles], Phaneuf et al. (1978) [filled circles], Meyer et al. (1979) [filled square]. Previous theory: Rapp & Ortenburger (1960), SC [thin dot-dashed line]; Eichler et al. (1981), OBK [thin long dashed line]; Janev & McDowell, CTMC (1984) [open diamond]. Recommended cross section: Janev et al. (1995) [thin dashed line]
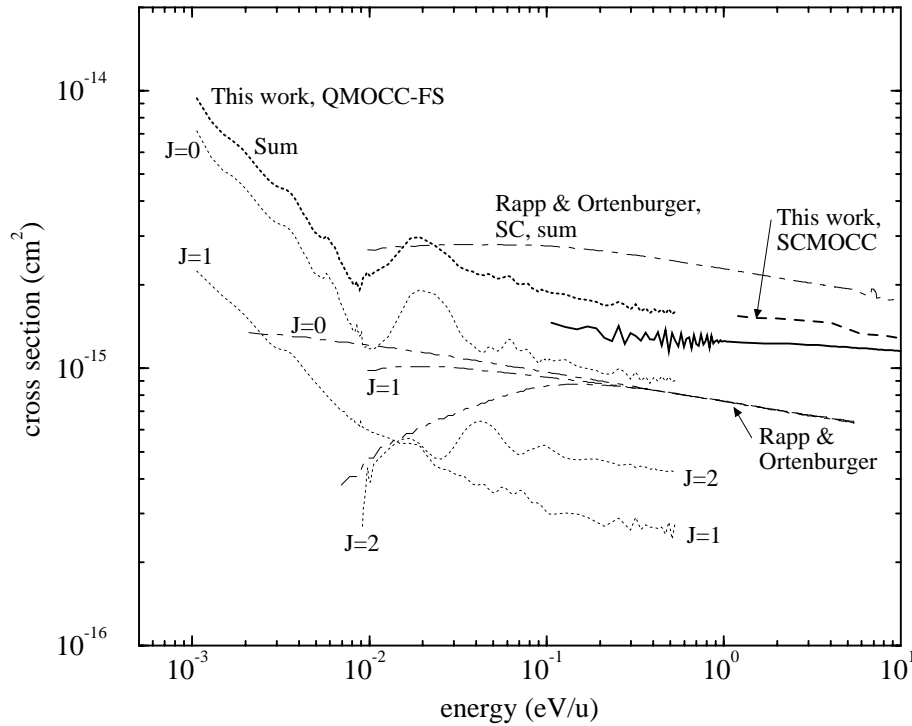

Fig. 2. Fine-structure resolved charge transfer cross sections for reaction (1), O$^+$ + H → O + H$^+$. Symbols same as Fig. 1, with additions. Fine-structure resolved: this work, QMOCC-FS [thin dotted lines]; Rapp & Ortenburger (1960), SC [thin dot-dashed lines]
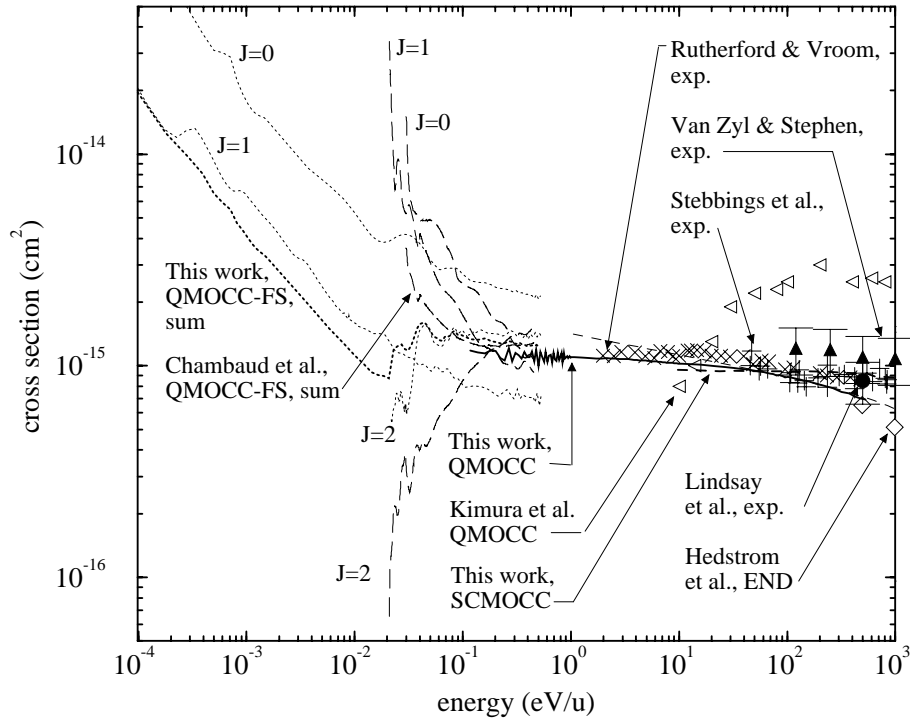
Fig. 3. Total charge transfer cross sections for reaction (2), H$^+$ + O → H + O$^+$. This work: QMOCC [thick solid line], QMOCC-FS [thin dotted line, J-resolved; thick dotted line, statistical averaged sum], SCMOCC [thick dashed line]. Previous experiment: Stebbings et al. (1964) [pluses], Rutherford & Vroom (1974) [X's], Van Zyl & Stephen (1992) [filled up triangles], Lindsay et al. (1996) [filled circles]. Previous theory: Chambaud et al. (1980), QMOCC-FS [thin long dashed lines, J-resolved and statistical averaged]; Kimura et al. (1997), QMOCC [open left triangles]; Hedström et al. (1998), END [open diamonds]. Recommended cross section: Janev et al. (1995), by detailed balance [thin dashed line]

calculation of Rapp & Ortenburger appears to over-estimate the cross section by a factor of ∼ 2 between 0.1 eV/u and 1 keV/u and has the wrong energy dependence for lower energies.

For higher energies, Fig. 1 displays new CTMC and CDW results compared to the experiments of Phaneuf et al. (1978) and Meyer et al. (1979), the Oppenheimer-Brinkman-Kramers (OBK) approximation calculation of Eichler et al. (1981), and the CTMC calculation of Janev & McDowell (1984). For collision energies greater than 20 keV/u and 500 keV/u, the current CTMC and CDW results, respectively are in good agreement with the previous measurements and calculations. As mentioned earlier, CTMC is not reliable at lower energies because it neglects quantum tunneling effects.

For lower energies (< 0.5 eV/u), the fine-structure of the oxygen atom becomes important. Our new QMOCC-FS fine-structure resolved and total cross sections for reaction (1) are displayed in Fig. 2. The only data available for comparison are the semiclassical calculations of Rapp & Ortenburger (1960) which are in significant disagreement with the current results. The current total QMOCC-FS is in good agreement with the current QMOCC and SCMOCC between 0.1 and 1 eV/u.

Cross sections for reaction (2), H$^+$ + O, are presented in Figs. 3 and 4. In Fig. 3 the new QMOCC computa-

tions are compared to the experiments of Stebbings et al. (1964), Rutherford & Vroom (1974), Van Zyl & Stephen (1992), and Lindsay et al. (1996), the QMOCC-FS calculations of Chambaud et al. (1980), the QMOCC results of Kimura et al. (1997), the electron nuclear dynamics (END) calculations of Hedström et al. (1998), and the cross section deduced by detailed balance from the recommended reaction (1) cross section of Janev et al. (1995). The current QMOCC is in good agreement with the experimental data for energies less than about 200 eV/u. The discrepancy at higher energies may be related to our neglect of ETFs. For energies greater than 10 eV/u, the current SCMOCC results, which include ETFs, are in excellent agreement with the experimental data, while the END calculation underestimates the data. The previous QMOCC calculation of Kimura et al. (1997) neglected the initial approach degeneracy factors and apparently used an integration step size which was too large.

At lower energies, Fig. 3 displays the current fine-structure resolved QMOCC-FS results and those of Chambaud et al. Near 0.1 eV/u the two calculations are in reasonable agreement, but appear to diverge for lower energies with the current results for $J = 0$ and $J = 1$ following the expected $1/v$ behavior. The Chambaud et al. cross sections have a much steeper low-energy dependence. The statistically averaged sum
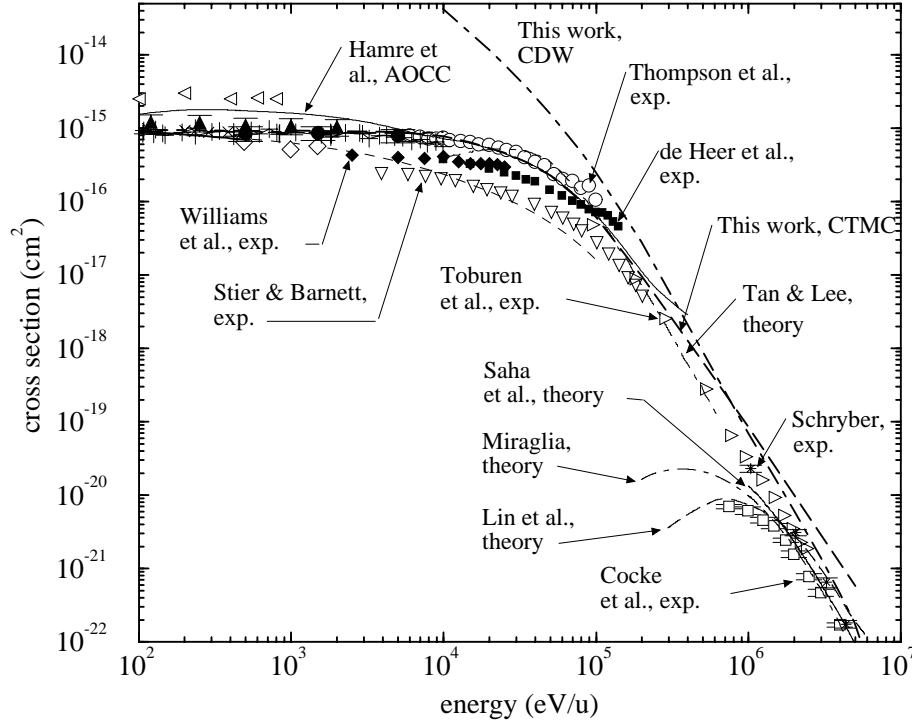
Fig. 4. Same as Fig. 3, but with additions. This work: CTMC (all shells) [thick long dashed line], CDW (all shells) [thick dot-dash line]. Previous experiment: Stiers & Barnett (1956) [open down triangle], de Heer et al. (1966) [filled squares], Schryber (1967) [stars], Toburen et al. (1968) [open left triangles], Cocke et al. (1977) [open squares], Williams et al. (1984) [filled diamonds], Thompson et al. (1996) [open circles]. Previous theory: Hamre et al. (1999) [thin solid line], Lin et al. (1978) [thin long dashed line], Tan & Lee (1981) [thin dot-dash line], Miraglia (1984) [thin dot-dash line], Saha et al. (1985) [thin solid line]

of the fine-structure cross sections agree between 0.1 and 0.5 eV/u, but again diverge for lower energies. While the differences in the magnitudes of the cross sections may be related to differences in the radial coupling matrix element (not explicitly given by Chambaud et al.), we cannot explain the lower energy discrepancies.

Figure 4 shows reaction (2) cross sections for energies greater than 100 eV/u. The current CTMC and CDW calculations (which include the sum of capture from the O(1s), O(2s), and O(2p) subshells computed using the independent electron model) are compared with the experiments of Stier & Barnett (1956), de Heer et al. (1966), Schryber (1967), Toburen et al. (1968), Williams et al. (1984), and Thompson et al. (1996), and the calculations of Tan & Lee (1981), and the atomic-orbital close-coupling (AOCC) results of Hamre et al. (1999). Additionally, the K-shell capture (i.e., removal of an O(1s) electron) measurements of Cocke et al. (1977) are compared to the theoretical calculations of Lin et al. (1978), Miraglia et al. (1984), and Saha et al. (1985). Other K-shell capture calculations (not shown for clarity) were performed by Ghosh et al. (1987), Belkić (1988), Dunseath et al. (1988), Gravielle & Miraglia (1988), and Kuang (1991). The CTMC results are in fair agreement with the experimental data. Unlike for reaction (1), CTMC is in good agreement with the measured cross sections from 1 to
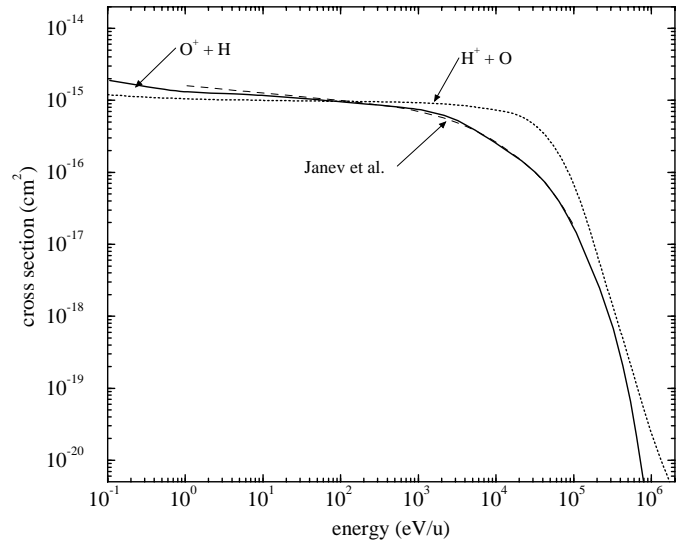

Fig. 5. Recommended total charge transfer cross sections. Reaction (1), O$^+$ + H → O + H$^+$: this work [thick solid line], Janev et al. (1995) [thin dashed line]. Reaction (2), H$^+$ + O → H + O$^+$: this work [thick dotted line]

300 keV/u. For $E > 300$ keV/u, it overestimates the total capture cross section because the K-shell contribution is calculated to be about a factor of three larger than the measurements of Cocke et al. (1977) (see Schultz &

Table 2. Cross section fit coefficients for Eq. (3)

Coefficient	Reaction (1)	Reaction (2)
a_1	$3.93\ 10^{-16}$	$1.20\ 10^{-15}$
a_2	$2.05\ 10^{-3}$	32.0
a_3	$7.16\ 10^{-2}$	$4.15\ 10^{-3}$
a_4	$2.95\ 10^{-8}$	$2.35\ 10^{-9}$
a_5	0.812	0.792
a_6	$3.01\ 10^{-2}$	$2.94\ 10^{-2}$
a_7	0.150	$7.26\ 10^{-3}$
a_8	0.183	$8.45\ 10^{-4}$
a_9	$1.04\ 10^{-2}$	$8.35\ 10^{-4}$
a_{10}	0.236	0.563

Stancil 1999). The current CDW results are in fair agreement with the measurements and the calculations of Tan & Lee (1981) for $E > 100$ keV/u, but are about a factor of two larger. However, we note that all of the high energy measurements were performed on O_2 targets except for Williams et al. and Thompson et al., with the O target assumed to be one-half of the O_2 cross section.

A new recommended cross section for reaction (1) was constructed through a non-linear fit of all the available data, but with exclusion of the calculations of Rapp & Ortenburger (1960) and the lower energy portions of the Phaneuf et al. and CDW results. The new recommended cross section is shown in Fig. 5 with fit coefficients for the relation

$$\sigma(E_3) = a_1 \left[\frac{\exp(-a_2/E_3)}{1 + a_3 E_3^2 + a_4 E_3^{4.5}} + a_5 \frac{\exp(-a_6 E_3)}{E_3^{a_7}} \right. $$
$$\left. + a_8 \frac{\exp(-a_9 E_3)}{E_3^{a_{10}}} \right] \quad cm^2 \tag{3}$$

given in Table 2 for energies between 0.5 eV/u and 1 MeV/u and E_3 is in units of keV/u. The fit deviates from what we consider to be the most reliable data at any given energy by less than 10%. There are some slight departures from the recommended cross section of Janev et al. (1995) as shown in Fig. 5.

Assuming detailed balance, we deduced a "recommended" cross section for process (2) from the Janev et al. reaction (1) cross section as shown in Figs. 3 and 4. The deduced cross section does not reproduce the most recent results. Using a consistent set of experimental and theoretical data, we also constructed a recommended cross section for process (2) shown in Fig. 5 with fit coefficients given in Table 2.

Figure 6 displays various theoretical and experimental rate coefficients for reactions (1) and (2) with the current results obtained by averaging the new recommended cross sections over a Maxwellian velocity distribution. Using a Langevin orbiting approximation, Field & Steigman (1971) estimated the rate coefficients for temperatures up to 10000 K, while using their QMOCC-FS cross sections, Chambaud et al. obtained rate coefficients up to only 1000 K. There is significant discrepancy between these

Table 3. Fine-structure resolved charge transfer rate coefficients α (cm^3 s^{-1}) for process (1) and fit coefficients for Eq. (4)

T(K)	$J = 0$	$J = 1$	$J = 2$	Total
10	$9.46 - 15^a$	$9.59 - 11$	$2.97 - 10$	$3.93 - 10$
20	$1.22 - 12$	$9.46 - 11$	$2.82 - 10$	$3.77 - 10$
30	$5.94 - 12$	$9.10 - 11$	$2.52 - 10$	$3.49 - 10$
50	$2.11 - 11$	$8.94 - 11$	$2.42 - 10$	$3.52 - 10$
100	$5.73 - 11$	$9.15 - 11$	$2.66 - 10$	$4.15 - 10$
200	$1.04 - 10$	$9.93 - 11$	$3.13 - 10$	$5.17 - 10$
500	$1.71 - 10$	$1.20 - 10$	$4.01 - 10$	$6.91 - 10$
1000	$2.27 - 10$	$1.47 - 10$	$5.00 - 10$	$8.74 - 10$
2000	$2.93 - 10$	$1.85 - 10$	$6.31 - 10$	$1.11 - 9$
5000	$4.02 - 10$	$2.59 - 10$	$8.66 - 10$	$1.53 - 9$
10000	$5.28 - 10$	$3.44 - 10$	$1.14 - 9$	$2.01 - 9$
b_1	$4.47 - 10^b$	$3.29 - 10$	$1.14 - 9$	$2.08 - 9$
c_1	$2.57 - 1$	$4.55 - 1$	$3.97 - 1$	$4.05 - 1$
d_1	$-5.49 + 4$	∞	∞	∞
b_2	$1.03 - 11$	$1.97 - 11$	$1.38 - 11$	$1.11 - 11$
c_2	$-3.65 - 1$	$-2.09 - 1$	$-2.98 - 1$	$-4.58 - 1$
d_2	85.7	$3.22 + 4$	$3.64 + 4$	∞

[a] The notation $A - B$ corresponds to $A \times 10^{-B}$.
[b] Multiply the fit by the endothermicity factor $\exp(-99$ K/T$)$.

two calculations. Further, the $O^+ + H$ measurement of Federer et al. (1984) is in agreement with Chambaud et al. while the $H^+ + O$ measurement of Fehsenfeld & Ferguson (1972) is consistent with Field & Steigman (1971). For reaction (1), our new total rate coefficients are consistent with Chambaud et al., but generally are slightly larger. The new results are also a factor of two larger than Field and Steigman at 10000 K. For reaction (2), the rate coefficients for a population of oxygen atoms in collisional equilibrium is only slightly larger than for the rate coefficients with all atoms in the $J = 2$ level for $T < 1000$ K. Both are only slightly smaller than the rate coefficients determined by Field and Steigman except at $T = 10000$ K, where the current results are a factor of 1.8 larger. The current reaction (2) rate coefficients are somewhat larger than the Chambaud et al. results. At high temperatures, the current rate coefficients are in fair agreement with Kimura et al. (1997) for reaction (2) for $T > 50000$ K. J-resolved rate coefficients are also displayed in Fig. 6.

The current rate coefficients are fit to the form

$$\alpha(T) = \sum_i b_i \left(\frac{T}{10\ 000} \right)^{c_i} \exp\left(\frac{-T}{d_i} \right) \quad cm^3/s \tag{4}$$

with the parameters b_i (cm^3 s^{-1}), c_i, and d_i (K) given in Tables 3 and 4 along with $\alpha(T)$ for several values of T. The fits do not deviate from the computed rate coefficients by more than $\sim 15\%$. For the J-resolved rate coefficients, the fits are only applicable for $T \leq 10000$ K. Higher temperature rate coefficients are given in Table 5.
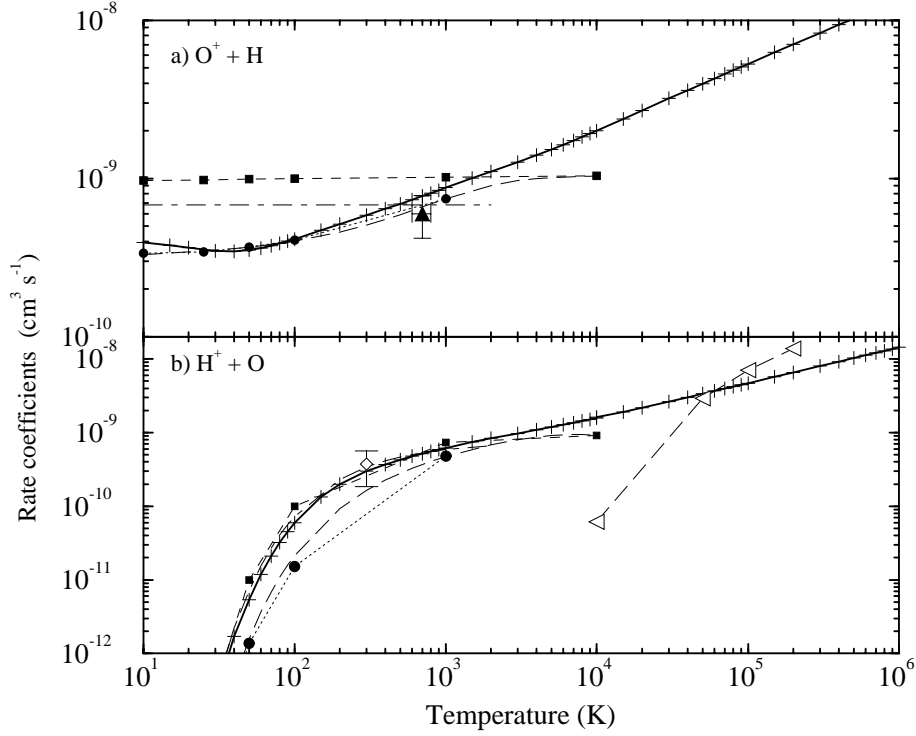
Fig. 6. Total charge transfer rate coefficients for **a)** Reaction (1), $O^+ + H \rightarrow O + H^+$ and **b)** reaction (2), $H^+ + O \rightarrow H + O^+$. This work: total for reaction (1) and collisional equilibrium for reaction (2) [thick solid lines with pluses]. Previous experiment: Fehsenfeld & Ferguson (1972) [open diamond], Federer et al. (1984) [filled up triangle]. Previous theory: Field & Steigman (1971) [squares with thin dashed lines], Chambaud et al. (1980) [circles with thin dotted lines], Kimura et al. (1997) [left triangles]. Recommended: Kingdon & Ferland (1996) [thin long dashed lines], Millar et al. (1997) [thin dot-dashed lines]

4. Applications

Because of the large abundances of hydrogen, oxygen, and their ions and the efficiency of the charge transfer reactions (1) and (2), the processes are important in a variety of astrophysical and atmospheric environments. They can influence the ionization balance, chemistry, radiative spectrum, cooling, and possibly heating of astrophysical plasmas.

4.1. The interstellar medium

Much of the chemistry in the interstellar medium is driven by ionization. However, atomic oxygen cannot be photoionized by the interstellar radiation field in either dense or diffuse interstellar clouds. The necessary source of ionization is provided by cosmic rays which collisionally ionize H to create H^+. The proton can then capture an electron from the oxygen atom via reaction (2) thereby initiating the oxygen chemistry. Most interstellar cloud models adopt the standard set of reaction rate coefficients given by Millar et al. (1997). For process (2) they suggest the relation $7.0 \ 10^{-10} \exp(-223/T)$ cm^3 s^{-1} shown in Fig. 6. This is based on the measurement of Fehsenfeld & Ferguson (1972) with the oxygen fine-structure levels
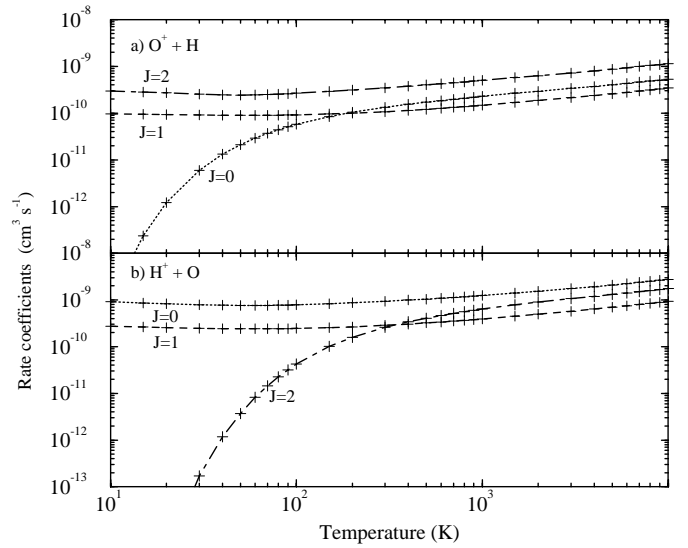

Fig. 7. J-resolved charge transfer rate coefficients for **a)** Reaction (1), $O^+ + H \rightarrow O + H^+$ and **b)** reaction (2), $H^+ + O \rightarrow H + O^+$

in collisional equilibrium. Black & Dalgarno (1977) deduced a similar value by modeling the OH and HD abundances in a diffuse interstellar cloud. The new reaction (2) rate coefficients are in good agreement with the earlier

Table 4. Fine-structure resolved charge transfer rate coefficients α (cm^3 s^{-1}) for process (2) and fit coefficients for Eq. (4)

T(K)	$J = 0$	$J = 1$	$J = 2$	Equil.
10	$9.17 - 10$	$2.71 - 10$	$3.17 - 20$	$5.21 - 20$
20	$8.21 - 10$	$2.56 - 10$	$3.59 - 15$	$5.33 - 15$
30	$7.89 - 10$	$2.48 - 10$	$1.70 - 13$	$2.48 - 13$
50	$7.65 - 10$	$2.42 - 10$	$3.70 - 12$	$5.41 - 12$
100	$7.83 - 10$	$2.45 - 10$	$4.25 - 11$	$5.94 - 11$
200	$8.67 - 10$	$2.65 - 10$	$1.59 - 10$	$1.98 - 10$
500	$1.04 - 9$	$3.21 - 10$	$4.06 - 10$	$4.29 - 10$
1000	$1.25 - 9$	$3.92 - 10$	$6.37 - 10$	$6.19 - 10$
2000	$1.53 - 9$	$4.95 - 10$	$8.97 - 10$	$8.34 - 9$
5000	$2.08 - 9$	$6.95 - 10$	$1.30 - 9$	$1.19 - 9$
10000	$2.74 - 9$	$9.32 - 10$	$1.75 - 9$	$1.59 - 9$
b_1	$2.39 - 9$	$7.91 - 10$	$1.57 - 9^a$	$1.26 - 9^a$
c_1	$3.27 - 1$	$3.11 - 1$	$2.98 - 1$	$5.17 - 1$
d_1	$-2.06 + 5$	$-5.97 + 5$	$-7.51 + 4$	∞
b_2	$3.54 - 11$	$1.96 - 11$	$1.62 - 7$	$4.25 - 10$
c_2	$-4.26 - 1$	-3.29	1.13	$6.69 - 3$
d_2	$5.27 + 3$	$2.21 + 2$	19.4	∞

[a] Multiply the fit by the endothermicity factor $\exp(-227 \text{ K}/T)$.

Table 5. Total charge transfer rate coefficients α (cm^3 s^{-1})

T(K)	Reaction (1)		Reaction (2)		
	a	b	c	d	b
10000	$2.01 - 9$	$1.4 - 9$	$1.61 - 9$	$6.1 - 11$	$9.1 - 10$
20000	$2.69 - 9$		$2.19 - 9$		
50000	$3.97 - 9$		$3.37 - 9$	$2.91 - 9$	
80000	$4.83 - 9$		$4.22 - 9$		
100000	$5.30 - 9$		$4.71 - 9$	$7.02 - 9$	
200000	$7.04 - 9$		$6.59 - 9$	$1.39 - 8$	
500000	$1.02 - 8$		$1.03 - 8$		
800000	$1.24 - 8$		$1.29 - 8$		
1 10^6	$1.36 - 8$		$1.44 - 8$		
2 10^6	$2.14 - 8$		$2.02 - 8$		
5 10^6	$2.61 - 8$		$3.11 - 8$		
8 10^6	$3.09 - 8$		$3.86 - 8$		
1 10^7	$3.31 - 8$		$4.27 - 8$		

[a] This work.
[b] Field & Steigman (1971).
[c] This work, determined from the fine-structure cross section as given in Table 2.
[d] Kimura et al. (1997).

estimates, though somewhat larger than the QMOCC-FS calculations of Chambaud et al., and should not have a significant effect on the oxygen chemistry. For process (1) Millar et al. suggest the constant value of $6.8 \ 10^{-10}$ cm^3 s^{-1} based on the measurement of Federer et al. (1984), which is also in agreement with the value deduced by Black & Dalgarno (1977). However, the new results and those of Chambaud et al. (1980) suggest the rate coefficient has a significant temperature dependence decreasing below the Federer et al. measurement for $T < 500$ K and as a result

may enhance the oxygen chemistry by reducing the O$^+$ removal efficiency.

4.2. Gaseous nebulae

O I and O II emission lines are observed in a variety of photoionized nebulae including classical novae (e.g., Andreä et al. 1994), planetary nebulae (e.g., Péquignot et al. 1978), H II regions (e.g., Baldwin et al. 1996), and metal line systems in high redshift clouds (e.g., Petitjean et al. 1996). Reactions (1) and (2) are important in establishing the O$^+$/O ratio, which because of the efficiencies of the charge transfer reactions tracks the H$^+$/H ratio. Given the available data, Kingdon & Ferland (1996) deduced a set of recommended rate coefficients from the Chambaud et al. (1980) data and an extrapolation to the 10000 K data of Field & Steigman (1971). Figure 6 shows that the current rate coefficients become greater than those of Kingdon & Ferland (1996) for $T > 2000$ K, being about a factor of two larger at 10000 K. This may have some effect on the oxygen ionization balance. Further, Kingdon & Ferland (1999) have suggested that in photoionized nebulae charge transfer can be an important heating mechanism. The reaction N$^+$ + H is the most important reaction, but process (1) can contribute about 2%. Use of the current rate coefficients in future photoionization models could enhance the effect of charge transfer on the thermal balance.

Péquignot (1990) performed an extensive study of the populations of the neutral oxygen fine-structure levels in gaseous nebulae. Adopting the rate coefficients of Chambaud et al., he was the first to include charge transfer in such an analysis. As he found that charge transfer had a critical influence on the fine-structure level populations, use of the current rate coefficients may modify his results for $T > 1000$ K.

4.3. The heliosphere

The interface between the solar wind and the local interstellar medium defines the heliopause which encloses the heliosphere. Because of the magnetic field of the heliosphere, interstellar O$^+$ cannot cross the heliopause, but instead moves along its outer surface. However, oxygen ions can charge exchange with H, via reaction (1), allowing the resulting neutral O atom to penetrate into the heliosphere. The neutral O atoms will eventually charge exchange with solar wind protons, via reaction (2), get accelerated and become part of the solar wind - so-called pick-up ions (e.g., Zank et al. 1999). Pick-up ions have been detected by the Ulysses spacecraft and may be a useful diagnostic of the local interstellar plasma. Heliospheric models by Izmodenov et al. (1997) suggest neutral O could penetrate to within 50 AU of the sun with the heliopause

crossing efficiency strongly influenced by the reaction (1) cross section.

4.4. The Jovian atmosphere

The discovery of soft X-ray emission from the Jovian aurora and measurements of energetic oxygen and sulfur ions from Io suggest that the ions are precipitating into the Jovian atmosphere and charge exchanging with the neutral atmospheric constituents H_2, H, and He. The electrons are captured into highly excited states of the highly charged ions which then radiate the X-rays (see Stancil et al. 1998c for a review). While X-rays will not be emitted by either O^+ or O, reaction (1) can play an important role in the deceleration of the energetic ions and the ionization stage distribution. Recent Monte Carlo calculations of oxygen ion beam stopping in the Jovian atmosphere were performed by Kharchenko et al. (1998). They found that a O^+ ion beam ensemble of 10 MeV would be quickly converted to an O^{8+} beam in less than 200 collision events. The charge and energy of the beam slowly decreases until after just $1.5 \, 10^5$ collisions when the beam becomes mostly O^+ with an energy of 1 MeV. The cross section shown in Fig. 1 is therefore relevant to the initial and final stages of the oxygen precipitation into Jupiter.

5. Summary

New theoretical calculations of charge transfer in collisions of O^+ with H and H^+ with O have been presented for collision energies between 0.1 meV/u and 10 MeV/u. Using these results in conjunction with previous experimental and theoretical data, accurate cross sections and rate coefficients have been computed which are applicable in numerous astrophysical and atmospheric situations.

References

Andreä J., Drechsel H., Starrfield S., 1994, A&A 291, 869

Baldwin J.A., et al., 1996, ApJ 468, L115

Bashkin S., Stoner J.O. Jr., 1975, Atomic Energy-Levels and Grotrian Diagrams. Amsterdam, North-Holland

Belkić D., 1988, Phys. Rev. A 37, 55

Belkić D., Gayet R., Salin A., 1984, Comp. Phys. Comm. 32, 385

Black J.H., Dalgarno A., 1977, ApJS 34, 405

Chambaud G., Launay J.M., Levy B., et al., 1980, J. Phys. B 13, 4205

Clementi E., Roetti C., 1974, At. Data 14, 177

Cocke C.L., Gardner R.K., Curnutte B., Bratton T., Saylor T.K., 1977, Phys. Rev. A 16, 2248

de Heer F.J., Schutten J., Moustafa H., 1966, Physica 32, 1766

Dunseath K.M., Crothers D.S.F., Ishihara T., 1988, J. Phys. B 21, L461

Eichler J.K.M., Tsuji A., Ishihara T., 1981, Phys. Rev. A 23, 2833

Federer W., Villinger H., Howorka F., et al., 1984, Phys. Rev. Lett. 52, 2084

Fehsenfeld F.C., Ferguson E.E., 1972, J. Phys. Chem. 56, 3066

Field G.B., Steigman G., 1971, ApJ 166, 59

Fite W.L., Smith A.C.H., Stebbings R.F., 1962, Proc. Roy. Soc. A 268, 527

Ghosh M., Mandal C.R., Mukherjee S.C., 1987, Phys. Rev. A 35, 2815

Gravielle M.S., Miraglia J.E., 1988, Phys. Rev. A 38, 5034

Hamre B., Hansen J.P., Kocbach L., 1999, J. Phys. B 32, L127

Hedström M., Deumens E., Öhrn Y., 1998, Phys. Rev. A 57, 2625

Izmodenov V., Malama Yu.G., Lallement R., 1997, A&A 317, 193

Janev R.K., McDowell M.R.C., 1984, Phys. Lett. A 102, 405

Janev R.K., Winter H.P., Fritsch W., 1995, in: Atomic and Molecular Processes in Fusion Edge Plasmas, Janev R.K. (ed.). Plenum Press, New York, p. 341

Kharchenko V., Liu W., Dalgarno A., 1998, J. Geophys. Res. 103, 26, 687

Kimura M., Lane N.F., 1990, Adv. At. Mol. Phys. 26, 79

Kimura M., Gu J.-P., Hirsch G., Buenker R.J., 1997, Phys. Rev. A 55, 2778

Kingdon J.B., Ferland G.J., 1996, ApJS 106, 205

Kingdon J.B., Ferland G.J., 1999, ApJ 516, L107

Krajcar-Bronic I., Uramoto S., Kimura M., et al., 1999 (in preparation)

Kuang Y.R., 1991, Phys. Rev. A 44, 1613

Lin C.D., Soong S.C., Tunnell L.N., 1978, Phys. Rev. A 17, 1646

Lindsay B.G., Sieglagg D.R., Schafer D.C., et al., 1996, Phys. Rev. A 53, 212

Meyer F.W., Phaneuf R.A., Kim H.J., Hvelplund P., Stelson P.H., 1979, Phys. Rev. 19, 515

Millar T.J., Farquhar P.R.A., Willacy K., 1997, A&AS 121, 139

Miraglia J.E., 1984, Phys. Rev. A 30, 1721

Olson R.E., Salop A., 1977, Phys. Rev. A 16, 531

Péquignot D., 1990, A&A 331, 499

Péquignot D., Aldrovandi S.M.V., Stasinska G., 1978, A&A 63, 313

Petitjean P., Riediger R., Rauch M., 1996, A&A 307, 417

Phaneuf R.A., Janev R.K., Pindzola M.S., 1987, in: Atomic Data for Fusion, Vol. 5, ORNL-6090

Phaneuf R.A., Meyer F.W., McKnight R.H., 1978, Phys. Rev. A 17, 534

Rapp D., Ortenburger I.B., 1960, J. Chem. Phys. 33, 1230

Roueff E., Dalgarno A., 1988, Phys. Rev. A 38, 93

Rutherford J.A., Vroom D.A., 1974, J. Chem. Phys. 61, 2514

Saha G.C., Data S., Mukherjee S.C., 1985, Phys. Rev. A 31, 3633

Schultz D.R., Stancil P.C., 1999 (in preparation)

Schryber U., 1967, Helv. Phys. Acta 40, 1023

Stancil P.C., et al., 1998a, ApJ 502, 1006

Stancil P.C., et al., 1998b, J. Phys. B 31, 3647

Stancil P.C., Krstić P.S., Schultz D.R., 1998c, in: Atomic Processes in Plasmas, Oks E., Pindzola M.S. (eds.). AIP, New York, p. 185

Stebbings R.F., Fite W.L., Hummer D.G., 1960, J. Chem. Phys. 33, 1226

Stebbings R.F., Smith A.C.H., Ehrhardt H., 1964, J. Geophys. Res. 69, 2349

Stier P.M., Barnett C.F., 1956, Phys. Rev. 103, 896

Tan C.K., Lee A.R., 1981, J. Phys. B 14, 2409

Thompson W.R., Shah M.B., Gilbody H.B., 1996, J. Phys. B 29, 725

Toburen L.H., Nakai M.Y., Langley R.A., 1968, Phys. Rev. 171, 114

Van Zyl B., Stephen T.M., 1992, in: Abstracts of Contributed Papers of the Seventeenth International Conference on the Physics of Electronic and Atomic Collisions, McCarthy I.E., MacGillivray W.R., Standage M.C. (eds.). Griffith, Brisbane, p. 437

Williams I.D., Geddes J., Gilbody H.B., 1984, J. Phys. B 17, 1547

Zank G., Lipatov A.S., Müller H., 1999, J. Geophys. Res. (submitted)

Zygelman B., Cooper D.L., Ford M.J., et al., 1992, Phys. Rev. A 46, 3846